Ciência eNatura, Santa Maria, v. 37 n. 2 jun. 2015, p. 162–172

ISSN impressa: 0100-8307 ISSN on-line: 2179-460X

Numerical Investigation Of Nanofluids Flow and Heat Transfer in 90° Elbow With square Cross-Section

Ayoob Khosravi Farsani [1], Afshin Ahmadi Nodooshan [2]

1. MS student in mechanical engineering, University of Shahrekord, Shahrekord
2. Assistant Professor of Mechanical Engineering, University of Shahrekord, Shahrekord

Abstract

In this article, forced convective heat transfer of nanofluid flow in a horizontal tube with a square cross-section and 90-degree elbow under heat flux was investigated in a numerical method. The homogeneous nanofluid of aluminum oxide and water (Al2O3) was used as the working fluid. For the numerical solution of continuity, momentum and energy equations, the finite volume method was used. In this study, the effect of Reynolds number and the solid volume fraction and the impact of the elbow on the flow field and the heat transfer rate and pressure drop was investigated. The results were presented in the form of flow and temperature contours and the Nusselt diagrams, which have a good relation with the experimental results, and showed that by increasing the solid volume fraction and Reynolds number, the heat transfer in the elbow increases. Also the concave surface from inside the tubes had a greater impact on heat transfer than the convex surface.

Keywords*: laminar flow, nanofluid, elbow 90 degrees, square cross-section, heat transfer*

1 INTRODUCTION

Undoubtedly, heat transfer is one of the most important and most widely used part of engineering science and its significance can be multiplied with respect to the energy crisis and the need for fuel savings. Low thermal conductivity of conventional heat fluids such as water, oils, … reduces the efficiency of heating equipment, so nowadays the new technology of nanotechnology has been able to help scientists to introduce the high-capacity thermal transmission systems called nanofluids. According to " the rule of higher thermal conductivity of fluid compared to metal", mixed metal nanoparticles suspended in nanofluid for increasing thermal conductivity of fluids and energy saving has taken the focus of nanomechanical studies.

Here among a lot of researches conducted on this flows, we refer to several cases. Among the first theory studies on the curved pipe, we can point to Mr. Dean research in 1927 [1]. He indicated that the flow dynamic in bends depends on Dean dimensionless parameter, which is in fact the ratio of inertial and centrifugal forces to viscous force.

Enayet et al [2] achieved speed in a 90-degrees elbow with square cross-section and ratio of radius to the channel width of 7 by Laser-Doppler. They drawn contour speed at different angles of elbow in the pipe section, and correspond to Reynolds, they provided average speed, turbulence intensity and shear stress in charts to predict the flow, and the results were used as the basis for turbulence models and computer software.

Mohammad Boutabaa et al [3] examined three-dimensional numerical simulation of secondary flows in developing flow and Newtonian fluid and viscoelastic in a curved duct of square cross-section. They conducted simulation for three different Dean numbers and using a discrete finite volume and an orthogonal coordinate system, and showed that in both Newtonian and non-Newtonian fluids, the size and numbers of vortices depend on Dean number, and by increasing the number, Dean length of development is reduced. The viscosity also affects on the secondary flow and the vortices growth rate in viscoelastic fluid is more than Newtonian fluid.

Taofik et al [4] in an experimental laboratory studied the characteristics of two nanofluids, Al_2O_3/water and CuO/water, in laminar flow in a square cupric duct and concluded that there is a significant increase of heat transfer in both nanofluids compared to base fluid; however CuO nanofluid showed better heat transfer than Al_2O_3 nanofluid.

Sasmito et al [5] in their article examined the numerical heat transfer by changing flow geometry and/or by enhancing thermal conductivity of the fluid. The purpose of this article was increasing the heat transfer fluid by simultaneous changing flow geometry and nanofluid in the quadrilateral cross-section pipes; and two nanofluids, i.e. water/Al_2O_3 and water/CuO have been studied. And also the amount of thermal conductivity from different geometries, such as straight pipes, flat-spiral pipe, cylindrical helix and bevel helical compared, which in result the heat transfer from flat-spiral geometry was more than others, as well as increasing 1 percent of nanofluid concentration led to a significant increase in heat transfer, and increasing of the solid particles is not recommended more than this amount.

Junhong Yang et al [6] experimentally compared the laminar flow of nanofluid in the curved and straight pipes and showed that in the straight pipes, at higher Reynolds numbers the particles concentration is high, while in the curved pipes, at higher Reynolds numbers we have lower concentration of the particles. It seems that by increasing the Reynolds number, the effect of bending in stability of suspended particles is increased; it can be concluded that by increasing the concentration of particles and reducing the curvature we can keep fluid in the higher Reynolds numbers.

Dongsheng et al [7] experimentally investigated convective heat transfer of $Al_2 O_3$ nanofluid flow inside a straight pipe under laminar flow and concluded that:

By using aluminum oxide nanoparticles in laminar flow, the convective heat transfer is increased and also the heat transfer is increased with the increase of the Reynolds number.This increase in heat transfer is significant especially in the entrance region and decreases with distance from the axis; and the length of thermal developed region in nanofluid is more than the base fluid, and it increases with the increase of the particle concentration.Displacement of these particles reduces the viscosity and reduces the thickness of the thermal boundary layer which causes increasing in convective heat transfer.

Alireza Akbari Nia et al [8] numerically simulated the laminar flow of nanofluid inside the horizontal pipe in three-dimensional state with respect to the effects of two centrifugal and buoyancy forces by using the finite-volume method. The research results showed that increasing solid nanoparticles volume has no effect on the axial velocity and frictional drag coefficient. Adding solid nanoparticles increases fluid temperature; it hasn't significant effects on secondary flow and also increases heat transfer. Increasing Grashof number increases secondary flow arised due to buoyancy force; therefore it leads to disturb the symmetry in the secondary velocity vectors and temperature contours and reduces the Nusselt number.

According to the literature, curved channels with a quadrilateral cross-section often used in energy facilities which are widely used in industrial devices, such as turbomachinery, cooling systems, air conditioning, heat exchangers, etc. But little research has been done in this regard; and since in these sections the pressure drop and heat transfer are very important, in this study we decided to examine laminar flow in a 90-degrees elbow with a quadrilateral cross- section.

2 Problem Statement

Figure 1 shows the computational region including curved pipe with axial angle θ between 0 and 90 degrees in the direction of constant wall heat flux. The curvature angle of the pipe is with a radius of R_c and its quadrilateral cross-section is to the side of h, which in the pipe nanofluids of water and aluminum oxide are flowing slowly and continuously at the entrance with the speed of v_0 and constant temperature of $T_0 = 298k$. In this figure L=300 mm ،h=80mm and $R_c = 160\,mm$. The non-uniform structured grid shown in Figure 2 is created for discretizing the computational region. Near the wall due to the high gradient of speed and temperature the grid is considered smaller. The sensitivity of the grid is examined with changing the number of nodes in different directions.

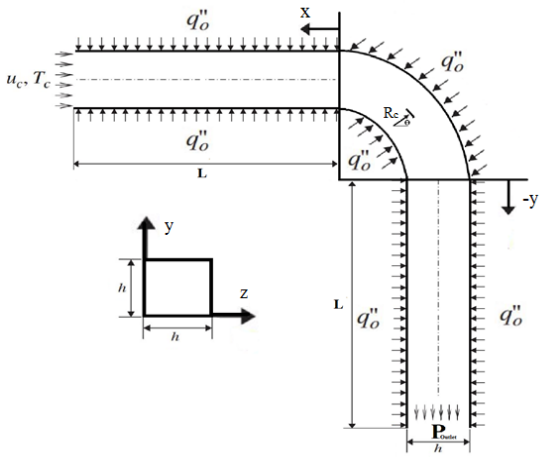

Figur 1: an overview of the geometry

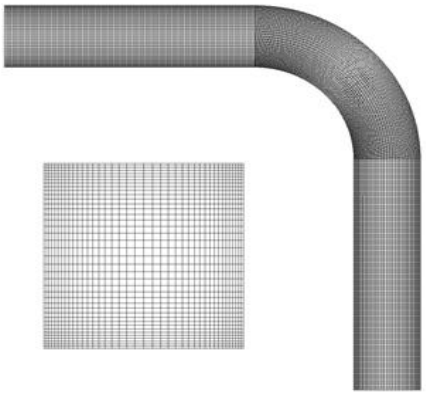

Figur 2: the computational grid

3 The basic equations governing the nanofluid flow

In this study, it is assumed that the nanofluid behaves as a homogeneous fluid and the flow of boundary layer is slow and stable [9] and is shown that nanofluids behave like the single-phase fluids [10]. Energy production is considered zero; and because nanoparticles' size is *extremely* small, it seems reasonable that the mixture can easily flow homogeneously inside the pipe. So we can ignore sliding motion between the phases and consider nanofluid as a continuum environment with thermal equilibrium between the base fluid and solid particles. It is assumed that nanofluid is incompressible with constant physical properties, which all the properties are calculated based on inlet temperature fluid as reference. The work of expansion and viscous losses in the energy equation are ignored.

The governing equations of laminar flow inside the channel, assuming incompressible Newtonian fluid and using the Boussinesq Approximation are [11]:
(In the above equations subtitles are used as c= cool surface, f= fluid, h= gram level, m= average, nf= nanofluids, i =inlet conditions, s= solid, w= wall).
Continuity equation**:**

$$\frac{\partial u}{\partial x}+\frac{\partial v}{\partial y}+\frac{\partial w}{\partial z}=0 \qquad (1)$$

Where
x,y, are the Cartesian coordinates
u,v, and w are velocities in the x and y and (m/s) z
Momentum equation**:**

$$\left(U\frac{\partial U}{\partial X}+V\frac{\partial U}{\partial Y}+W\frac{\partial U}{\partial Z}=-\frac{\partial P}{\partial X}+\frac{\mu_{nf}}{\varrho_{nf}\upsilon_f}\frac{1}{Re}\left(\frac{\partial^2 U}{\partial X^2}+\frac{\partial^2 U}{\partial Y^2}+\frac{\partial^2 U}{\partial Z^2}\right)\right. \qquad (2)$$

$$\left(U\frac{\partial V}{\partial X}+V\frac{\partial V}{\partial Y}+W\frac{\partial V}{\partial Z}=-\frac{\partial P}{\partial Y}+\frac{\mu_{nf}}{\varrho_{nf}\upsilon_f}\frac{1}{Re}\left(\frac{\partial^2 V}{\partial X^2}+\frac{\partial^2 V}{\partial Y^2}+\frac{\partial^2 V}{\partial Z^2}\right)\right. \qquad (3)$$

$$U\frac{\partial W}{\partial X}+V\frac{\partial W}{\partial Y}+W\frac{\partial W}{\partial Z}=-\frac{\partial P}{\partial Z}+\frac{\mu_{nf}}{\varrho_{nf}\upsilon_f}\frac{1}{Re}\left(\frac{\partial^2 W}{\partial X^2}+\frac{\partial^2 W}{\partial Y^2}+\frac{\partial^2 W}{\partial Z^2}\right) \qquad (4)$$

Where
X,Y,Z are dimensionless coordinates (X = x/L, Y = y/L, Z = z/L)
U,V,W are dimensionless components of the velocity (U = u/u_i, V = v/v_i, W = w/ (w_i))
Re is Reynolds number, P = fluid pressure, ϱ = the fluid density (kg/m^3), υ =kinematic viscosity (m^2/s)
Energy equation**:**

$$\left(U\frac{\partial\Theta}{\partial X}+V\frac{\partial\Theta}{\partial Y}+W\frac{\partial\Theta}{\partial Z}\right)=\frac{\alpha_{nf}}{\alpha_f}\frac{1}{Re.Pr}\left(\frac{\partial^2\Theta}{\partial X^2}+\frac{\Theta}{\partial Y^2}+\frac{\partial^2\Theta}{\partial Z^2}\right) \qquad (5)$$

Where
$\boldsymbol{\Theta}$ is dimensionless temperature ($\Theta = T-T_c/T_h-T_c$)
α is thermal dispersion coefficient of fluid (m^2/s)
Pr is Prandtl number ($Pr=\upsilon_f/\alpha_f$)

The dimensionless variables used in the equations are defined as follows:

$$X=\frac{x}{L},\ Y=\frac{y}{L},\ Z=\frac{z}{L},\ U=\frac{u}{u_i},\ V=\frac{v}{v_i}$$

$$W=\frac{w}{w_i},\ \Theta=\frac{T-T_c}{T_h-T_c},\ P=\frac{\bar{p}}{\varrho_{nf}u_i^2}$$

$$Re=\frac{\varrho_f u_i L}{\mu_f},\ Pr=\frac{\upsilon_f}{\alpha_f}$$

4 Physical and thermal properties of nanofluids:

The following formulas have been used to study the physical and thermal properties of nanofluid:

Nanofluid effective density [12]:

$$\varrho_{nf}=(1-\varphi)\varrho_{f,o}+\varphi\varrho_{s,o} \qquad (6)$$

Effective heat capacity of nanofluid**:**

$$(C_p)_{nf}=\left[\frac{(1-\varphi)(\varrho C_p)_f+\varphi(\varrho C_p)_s}{(1-\varphi)\varrho_f+\varphi\varrho_s}\right] \qquad (7)$$

The effective thermal conductivity and dynamic viscosity of nanofluid provided by Ravikanth and Debendra [13] are as the following equations:
The effective thermal conductivity of nanofluids:

$$K_{nf} = \frac{k_s+2k_f-2(k_f-k_s)}{k_s+2k_f+(k_f-k_s)\varphi} k_f + 5\times 10^4 \beta\varphi\varrho_f (C_p)_f \sqrt{\frac{kT}{\varrho_s d_s}} f(T,\varphi) \quad (8)$$

The effective dynamic viscosity of nanofluids:

$$\mu_{nf} = 5\times 10^4 \beta\varphi\varrho_f \sqrt{\frac{k_b T}{\varrho_s d_s}} f(T,\varphi) \quad (9)$$

$$f(T,\varphi) = (2.8217\times 10^{-2}\varphi + 3.917\times 10^{-3})\left(\frac{T}{T_0}\right) + (-3.0669\times 10^{-2}\varphi - 3.91123\times 10^{-3}) \quad (10)$$

$$\beta = 8.4407(100\varphi)^{-1.07304} \quad (11)$$

$$1\% < \varphi < 10\%$$

$$298k < T < 363k$$

d is diameter of solid particles (20×10^{-9}) (m), $C_p$is the specific heat (j/kgk), g= acceleration of gravity (m/s^2), k= thermal conductivity (w/m^2k), Nu = Nusselt number ($Nu = ql/k(T_w - T_c)$), q" = heat flux (w/m^2) , R_c = elbow's radius of curvature(m), L = dimensionless diameter of pipe, T = temperature (k), φ = Volume fraction of solid particles (%), and θ is the angle of curvature (degree)

Table 1: Properties of Water and aluminum oxide particles [14]

Materials	$\mu(pa.s)$	$C_p(\frac{J}{kgk})$	$\rho(\frac{kg}{m^3})$	$k(\frac{W}{mk})$
Water	0.000993	4182	998.2	0.613
aluminum oxide	------	765	3970	40

5 Initial conditions and boundary conditions

To get the unique solution of a partial differential equation, a set of additional conditions are needed to determine optional functions resulting from the integration of partial differential equations. Mentioned conditions are divided as boundary conditions and initial conditions. In stability problems equations merely requires boundary conditions.

In this problem we have used constant wall flux boundary condition on the pipe walls because it has many applications in energy facilities; And also at the entrance we have used Velocity inlet boundary condition due to incompressible flow and at outlet we have used Pressure outlet boundary condition to prevent backward flow. A list of applied boundary conditions have been identified in Table 2.

Table 2: boundary conditions

name	type	Boundary conditions
entrance	Velocity inlet	w=v=0, u=1
outlet	Pressure outlet	P = 0
pipe wall	wall	u=v=w=0, $q = -k\left(\partial T/\partial r\right)$

6 Numerical Methods

Equations of continuity, momentum and energy with mentioned boundary conditions

were forced according to the finite difference method based on the finite volume. These equations were solved by Fluent Software; and the heat transfer coefficient and the effective dynamic viscosity were defined by open source (UDF) written for software. Second order upwind is used to discrete displacement and governing equations. The momentum equations are solved on the displaced grid. In displaced grid, addition to easily calculate the rate of flow on volume control, due to given speed on surface, the amount of pressure is determined on main point of grid. SIMPLE algorithm has been used to solve algebraic equations; it is described in detail in reference [15]. The convergence criterion is considered as the residual of velocities which is smaller than 10^{-6} at each stage. Three-dimensional geometry with quadrilateral is modeled by Gambit software and is used for simulation.

7 Verification of written code

To demonstrate the effectiveness of the method and written program, a comparison has been carried out between numerical results and similar works by others. To evaluate computer program performance developed in problems of nanofluid convective heat transfer in curved pipes, a comparison on nanofluid flow in an elbow was performed according to [16]. In this investigation, a 180-degree circular elbow is exposed to the heat flux while a nanofluid is flowing inside it. In this validation study, changes of average Nusselt number ratios of the nanofluid to the base fluid were investigated with increasing nanoparticles concentration in different Reynolds numbers. As indicated in Fig. 3a, there is a very small difference between the results of reference [16] and the results of the program. To evaluate the performance of the program in flows inside the quadrilateral cross-section pipe, its results are compared and analyzed with done work in reference [17]. In the above problem the air with temperature of $T_c = 298$ enters to a square cross-section 90-degree elbow and the wall is at the temperature of $T_h = 313$. In Table 3 the average Nusselt number rate that obtained from present study is compared with experimental results of reference [17]. As you can see, the results are reasonable and acceptable. (Dean Number $\left(\mathrm{Re}(a/2R_c)^{1/2}\right)$).

Table 3: Validation

Error Percent	Average Nusselt number		Dean number
	Present work	**Refrence result**	
6.12	8.703	8.17	200
1.94	11.779	11.55	400
1.11	14.13	14.289	600
2.77	16.123	16.584	800
3.62	17.878	18.551	1000

To select the grid right solution for present geometry, an investigation was conducted on the number of grid points. For this purpose, the effect of grid points' number on average Nusselt number is determined that indicates the rate of heat transfer from the hot walls of the channel. An example of conducted examinations is shown in Figure 3. In this figure we can see changes of average Nusselt number of fluid flow in a square cross-section 90-degrees elbow in Reynolds 100, based on the number of grid points. It should be noted that the average Nusselt number as an affected parameter by the number of grid points is suitable for this study. According to Figure 3b, it is clear that almost for grids which the number of nodes is more than 654360, the answers is remained in the same and significant changes in values are not seen. Thus, according to the studies and the implementation time, a uniform grid with 654000 nodes number was selected to run the program.

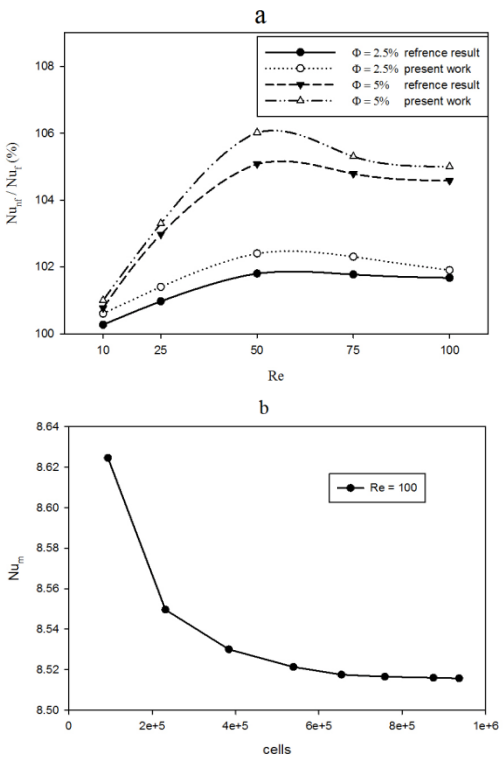

Figur 3

8 Results and discussion:

After selecting the appropriate grid and ensuring the validity of written code, governing equations were solved with the boundary conditions. Speed, temperature and pressure are obtained throughout flow field; and using the definition of Nusselt number, the heat transfer, pressure drop and Dimensionless speed are investigated in different elbow cross-sections at different Reynolds numbers and different volume ratio.

Local Nusselt number curves on the inner wall of elbow for a given amount of heat flux and constant Reynolds is shown in Fig. 4. Because of the convex inner wall, the thickness of the boundary layer begins to increase and the speed reduces near the wall. For this reason Nusselt number reduces to the minimum at the angle of 50 degrees. After the angle of 50-degree secondary flows are formed and because of this, after a fluctuation in Nusselt number it continues its downward trend until the end of the pipe.

Increasing the volume ratio of solid-liquid at a constant Reynolds increases the Nusselt number. Because with the increase of volume ratio, density increases according to equation (6), so to keep Reynolds, the speed should be increased. Thus increasing the solid-liquid volume ratio with increasing speed increases the heat transfer and Nusselt number.

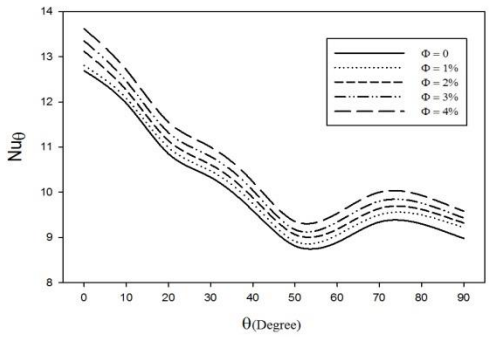

Figur 4: the local Nusselt number on the inner wall of the elbow in Re = 500 and q" = 2500 (w/m²)

In Fig. 5, the curves of local Nusselt number on the outer wall of elbow for a certain amount of heat flux and constant Reynolds is shown. It can be seen that in contrast to the inner wall, the Nusselt number increases due to a simultaneous effect of buoyant force and centrifugal force. At the angle of 50 degrees this upward trend decreases by forming the secondary flows. But in 70 degrees gradient gets higher again.

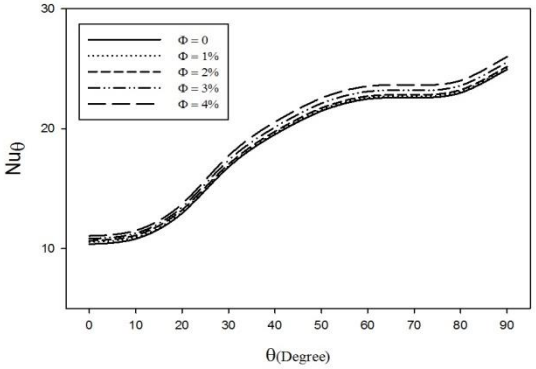

Figur 5: the local Nusselt number on the outer wall of the elbow in Re = 500 and q" = 2500 (w/m²)

In Fig. 6, the curves of local Nusselt number on the outer wall of elbow for a given amount of

heat flux and constant volume ratio is shown. As we see, with increasing Reynolds number the Nusselt number increases because of increasing speed, but through along the elbow with reducing the thickness of the boundary layer the Nusselt number increases due to the centrifugal force; and in higher Reynolds this upward trend decrease after angle of 40 degrees because of forming secondary flows.

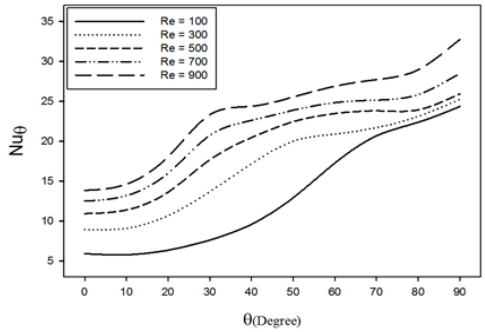

Figur 6: the local Nusselt number on the outer wall of the elbow in
$\varphi = 4\%$ and q" = 1500 (w/m²)

The curves of local Nusselt number on the inner wall of elbow for a given amount of heat flux and constant volume ratio is shown. As you can see in Fig. 7 , by increasing the Reynolds number like external wall, the Nusselt number increases; and during the elbow this Nusselt number at lower Reynolds numbers are declining due to increasing boundary layer thickness, and this decline is with a swing at higher Reynolds because of the formation of secondary flows.

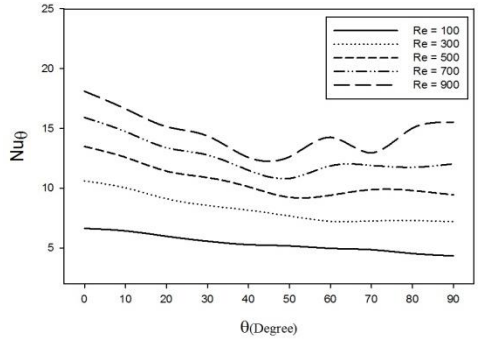

Figur 7: the local Nusselt number on the inner wall of the elbow in
$\varphi = 4\%$ and q" = 1500 (w/m²)

The diagram of pressure drop between elbow input and output at Reynolds numbers and in different volume ratio is drawn in Figure 8. It is observed that when the Reynolds number increases, the pressure drop becomes more because of increasing secondary flows; and also by increasing the volume ratio of solid particles according to equation (6), the density increases and thus the pressure drop becomes high too.

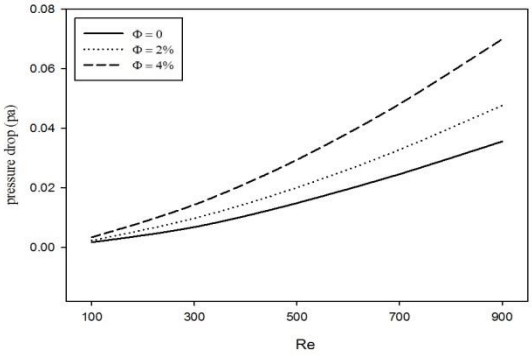

Figur 8: the elbow pressure drop

Fig. 9, shows the dimensionless axial velocity profile in cross-section perpendicular to the pipe at the angle of 90 degrees. As it expected, the speed on two walls is zero; and because of the centrifugal force, diagrams have a maximum value near the outer wall. By increasing the Reynolds number and the creation of secondary flow, this maximum value is inclined towards the center of the pipe.

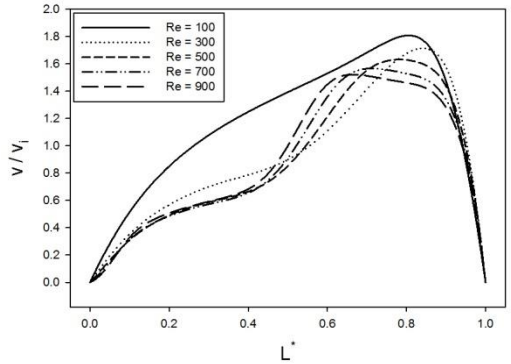

Figur 9: the dimensionless axial velocity profile in cross-section perpendicular to the pipe at the angle of 90 degrees

The cantor of flow dimensionless velocity is drawn in the cross-section of the pipe. Fig. 10 shows how the boundary layer is formed in input length, secondary flows, return flows in the elbow and the output length. According to this figure we can see that the fluid velocity is growing from input to Output; and at the output the flow is developed; and speed is higher near the outer wall.

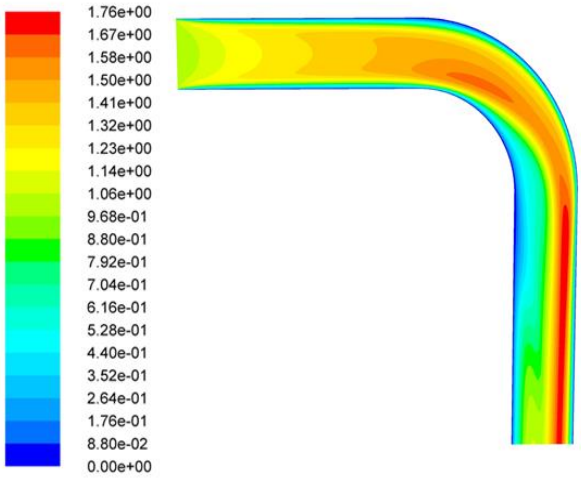

Figur 10: The cantor of dimensionless velocity in the cross-section of the pipe in q" = 2500 (w/m²) and φ = 4% and Re = 500

The contours of fluid dimensionless temperature at different cross sections of channel are shown in Fig. 11 (it shows upper side of the outer wall and lower side of inner wall). The dimensionless is defined as follows:

$$T^* = \frac{T - T_i}{T_i} \qquad (12)$$

In the above equation T is the temperature at any point of fluid and T_i is input fluid temperature to the pipe. Referring to the figure we can see that increasing in temperature occurs in the thin areanear to outer wall which is as the result of external heat flux. When the flow extends from cross- section with the angle θ = 30 ° to the cross- section with the angle θ = 90 ° , the vortex vicinage in the near of inner wall ,so that the area with high-temperature has transmitted gradually to the external wall. And also temperature contours are be changing to the end of pipe because the constant heat flux is inserted to the wall to the end of pipe.

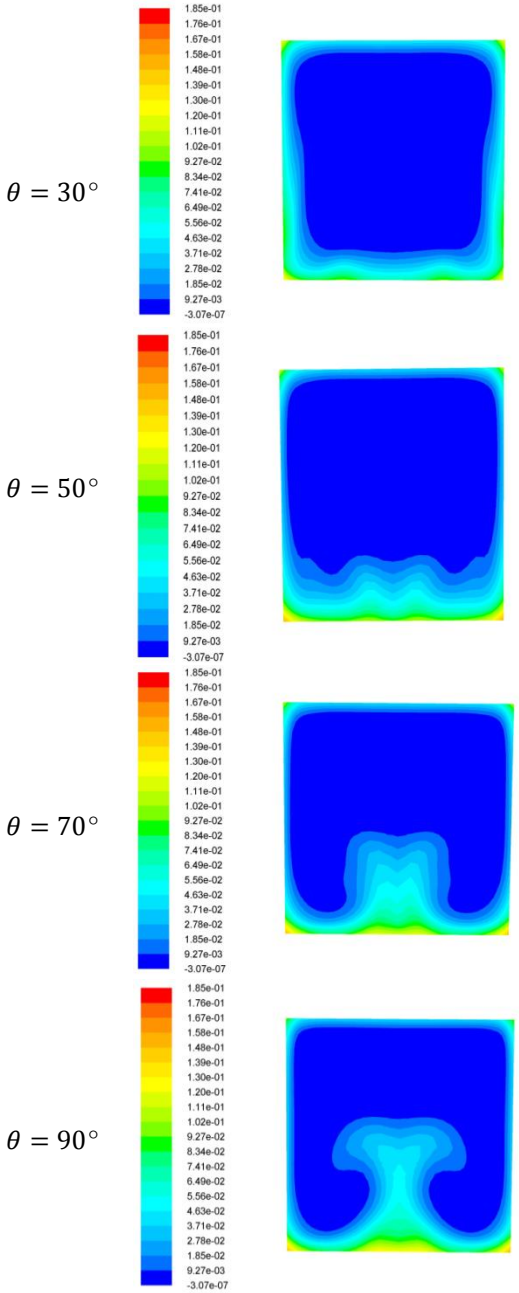

Figur 11: the dimensionless contours at angles of 30, 50, 70 and 90 degrees of elbow q" = 2500 (w/m²) and φ = 4% and Re = 700

Fig. 12, shows the dimensionless velocity contours (the ratio of speed at each cross-section to input speed) in sections with different angles elbow (the upper side is the outer wall and

lower side is the inner wall). Due to these figures, the secondary flow after the angle of 50 degrees begins to form. Because of the low bend, the flow is not developed in elbow length.

Also high speed area is inclined toward the outer wall and the low speed area is transferred to the central part of the cross section. These changes are due to the centrifugal force.

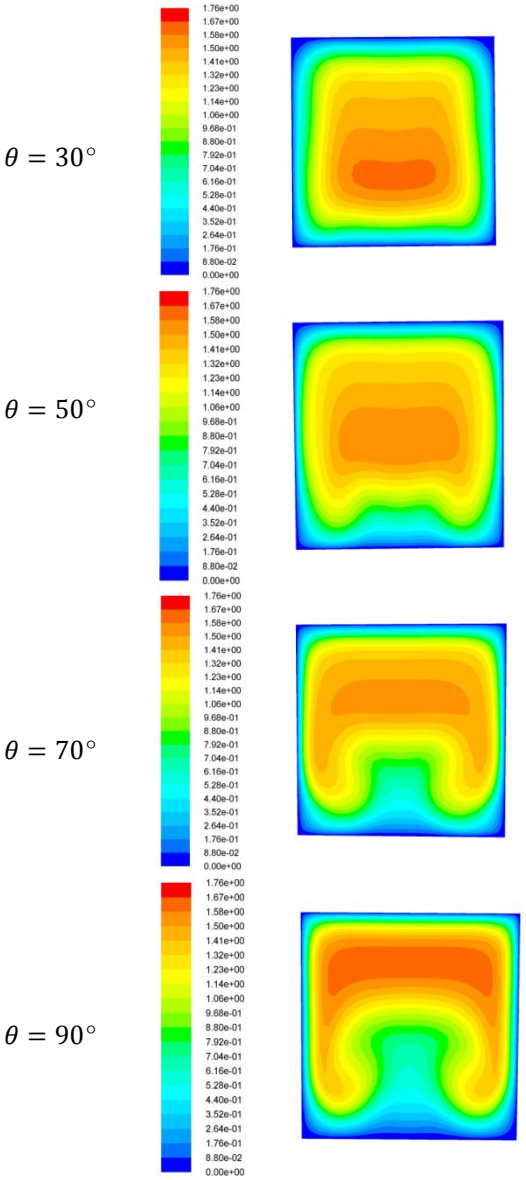

Figur 12: the velocity dimensionless contours at angles of 30, 50, 70 and 90 degrees of elbow q" = 2500 (w/m²) and φ = 4% and Re = 700

9 Conclusion

laminar and steady flow of nanofluid inside a pipe with a 90 degree elbow and the square cross-section were studied with considering the effects of two buoyancy and centrifugal forces in the three-dimensional state with numerical simulation by the Fluent software. It was found that by increasing the buoyancy force, the symmetry in the speed and temperature contours is omitted, while it delays development of axial velocity. In a given Reynolds number and constant heat flux, increasing the volume ratio of solid nanoparticles, increases the Nusselt number and the fluid temperature but there is no significant effect on the secondary flows. It was also observed that the inner wall plays little role in transferring heat as compared to the outer wall, that is due to the creation of secondary flows on the inner wall. It was observed that increasing two parameters of Rynoldz number and concentration of nanoparticles increases the pressure drop due to increasing secondary flows and density.

REFERENCES

Dean,W.R. (1927),"Not on the motion of fluid in a curved pipe",Phil.Mag.,l4,pp.208-.223.

Enayet, M. and Gibson M. M. and Yianneskis M. (1982)," Measurements of turbulent developing flow in a moderately curved square duct",Mechanical Engineering Department, Imperial College of Science and Technology

Mohammed, B. and Lionel, H. Gilmar, M. and Laurent, T. (2008) ," Numerical study of Dean vortices in developing Newtonian and viscoelastic flows through a curved duct of square cross-section",C. R. Mecanique, Vol. 337,pp. 40-47.

Taofik, H. and Nassan, S. and Zeinali, H. and Noie, S.H. (2010)," A comparison of experimental heat transfer characteristics for Al2O3/water and CuO/water nanofluids in square cross-section duct",International communication in heat and mass transfer, vol. 37, pp. 924-928.

Agus, P. S. and Jundika, C. K. and Arun, S. M. (2011),” Numerical evaluation of laminar heat transfer enhancement in nanofluid flow in coiled square tubes”,Department of Mechanical Engineering, National University of Singapore, 6:376

Junhong, Y. and Dapeng, C. and Qianqian D. (2011),” Effect of elbows on stability of water-baced TiO2 nanofluids under laminar flow conditions”,Proceedings of the ASME Power Conference

Dongsheng, W. and Yulong, D. (2004),” Experimental investigation into convective heat transfer of nanofluids at the entrance region under laminar flow conditions”, International journal of heat and mass transfer, vol. 47, pp. 5181-5188

Akbary nia, AR, (2007)"the development of nanofluid laminar flowinside the curved pipes with constant heat flux", , the Fifteenth Annual Conference (International) Mechanical Engineering, ISME2007_1827

Putra, N. and Roetzel, W. and Das, S. K. (2003),” Natural convection of nanofluids”, J. Heat Mass transfer,vol.39,pp.775-784.

Pak, B. C. and Cho, Y. I. (1998),” Hydrodynamic and heat transfer of dispersed fluid with submicron metallic oxide particles”, Exp. Heat transfer, vol. 11, pp. 151-170

Sadeghi. S, Ghasemi, B., (2013). "Mixed convection heat transfer of nanofluids in adiagonal channel under magnetic field", Journal of mechanical engineering lecturer, Volume 13, Issue 7, pp.18.

Haddad, Z. and Oztop, H. F. and Abu-Nada, E. (2012),” A review of natural convective heat transfer of nanofluids”, Renewable and sustainable energy reviews, vol. 16, pp. 5363-5378.

Vajjha, R. S. and Das, D. K. (2009),” Experimental determination of thermal conductivity of three nanofluids and development of new correlations”, International journal of heat and mass transfer, vol. 52, pp. 4675-4682.

Abu-Nada, E. and Masoud, Z. and Hijazi, A. (2008),” Natural convection heat transfer enhancement in horizontal concentric annuli using nanofluide”, Intrnational communications in heat and mass transfer,vol. 35, pp. 657-665.

Patankar, S. V. (1980),” Numerical heat transfer and fluid flow”, Hemisphere, washington, D.C.

Choi, J. and Zhang, Y. (2012),” Numerical simulation of laminar forced convection heat transfer of Al2O3-water nanofluid in a pipe with return bend”, International journal of thermal sciences,vol. 55, pp. 90-102.

Ojha, R. K. and Joshi, P. V. (2014),” Numerical analysis of forced convection and heat transfer in curved duct”, International journal of recent trends in mechanical engineering, vol. 2, pp. 2347-7326.